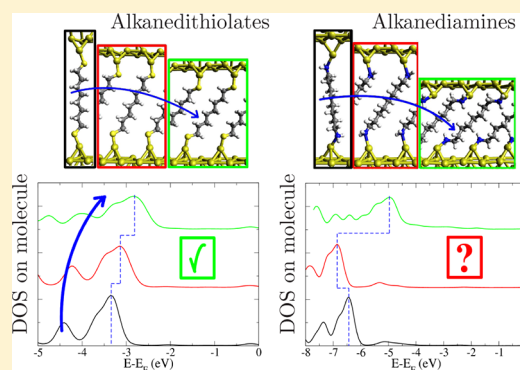


Interface Dipole Effects as a Function of Molecular Tilt: Mechanical Gating of Electron Tunneling through Self-Assembled Monolayers?

Giuseppe Foti,^{*,†,‡} Daniel Sánchez-Portal,^{†,‡} Andrés Arnau,^{†,‡,¶} and Thomas Frederiksen^{‡,§}[†]Centro de Física de Materiales, Centro Mixto CSIC-UPV, Paseo Manuel de Lardizabal 5, Donostia-San Sebastián, Spain[‡]Donostia International Physics Center (DIPC), Paseo Manuel de Lardizabal 4, Donostia-San Sebastián, Spain[¶]Depto. de Física de Materiales UPV/EHU, Facultad de Química, Apdo. 1072, Donostia-San Sebastián, Spain[§]IKERBASQUE, Basque Foundation for Science, E-48011, Bilbao, Spain

ABSTRACT: Control of electron transport through molecular devices is a fundamental step toward design of functional molecular electronics. In this respect, the application of the field-effect transistor principle to molecular junctions appears to be a desirable strategy. Here we study the possibility of mechanically controlling the molecular orbital alignment in self-assembled monolayers via the electrostatic fields originating from dipoles at the metal–molecule interfaces. More specifically, we analyze first-principles simulations of prototype alkanedithiolate and alkanediamine monolayer junctions between Au(111) electrodes as a function of inclination of the molecules in the film. We find that the molecular orbital alignment and hence the low-bias conductance of the junctions, sensitively depends on the interface dipole. The dipole change with molecular tilt is rationalized in terms of two electrostatic effects: (i) the reorientation of a dipole associated with the anchoring group and (ii) a dipole modification arising from charge redistribution due to the metal–molecule bond. The first effect, dominating for the thiolates, is the desired way to gate the junctions by tuning of the molecular tilt. However, the second effect, equally important for the amines, may hamper the mechanical control of the level alignment because it depends on other geometric details than the tilt angle. Our results thus suggest that mechanical gating by tilt is achievable with molecules and anchoring groups with strong intrinsic dipole moments and well-defined binding geometry rather than with interface dipoles associated with weak and flexible metal–molecule bonds.



■ INTRODUCTION

Since the first proposal¹ of a single-molecule electronic rectifier in 1974 many advances in the field of nanotechnology have led to the fabrication of various molecular devices² exhibiting similar functionality as components encountered in ordinary microelectronics, such as rectification,³ negative differential resistance,⁴ and switching.⁵ In addition to the efforts of chemical assembly of molecular electronic circuits, techniques have also been developed to construct single-molecule devices that display basic physical transport phenomena such as quantized conductance⁶ and Coulomb charging effects.⁷ However, detailed control of atomic contact geometry and molecular conformation is often difficult to achieve at the single-molecule level. To this extent, molecular self-assembly on metal surfaces is a convenient way to obtain well-characterized monolayer structures.^{8–10}

Alkanes, simple saturated carbon chains, bridging metal electrodes have been the prototype tunnel junction for investigating the electronic and transport properties across molecule–electrode interfaces.² These molecules have a large energy gap (of several electronvolts) between the highest occupied molecular orbital (HOMO) and the lowest unoccupied molecular orbital (LUMO). Notice that here and in the following, we reserve this nomenclature (HOMO and LUMO) to molecular orbitals that extend along the carbon alkane chain.

The presence of functional groups introduces additional levels in the molecular gap that are more strongly influenced by the interaction with the metal surface.

Alkane junctions display typical off-resonance transport characteristics as the Fermi energy E_F of the metal electrodes falls in the insulating HOMO–LUMO gap. The low-bias tunneling probability of electrons can therefore be understood in terms of an energy barrier, related to the position and alignment of the molecular level with respect to E_F , and of a tunneling length set by the number of methylene (CH_2) groups in the molecular backbone.

The conductance of alkane junctions has been shown to be sensitive to a number of details such as electrode shape and orientation,^{11,12} tilt and torsional angle of the molecule,^{13,14} and gauche defects.^{15,16} The alkane–metal interfaces also play decisive roles, as chemical anchoring groups differently affect the molecular level alignment and the contact resistance. The thiol group has been widely used as the anchoring element due to its extremely stable binding to gold, thus providing a good bench for comparing theoretical and experimental investiga-

Received: February 19, 2013

Revised: June 6, 2013

Published: June 7, 2013

tions.^{17–19} Alternatively, amine groups have been demonstrated to yield well-defined conductance values^{20–22} because the lone pair of amines binds preferentially to undercoordinated Au atoms, resulting in a flexible bond with well-defined electronic coupling between metal and molecule.^{22–26} Most recently, even alkanes with covalent Au–C contacts have been considered experimentally and theoretically.²⁷

The formation and structure of self-assembled monolayers (SAMs) has a long history in surface science.^{8–10} While alkanethiol is one of the most studied SAMs, alkanedithiols have also been shown to form ordered monolayers.²⁸ The ordering on surfaces is generally steered by the interplay between van der Waals intermolecule interactions and covalent molecule–substrate interactions. The former interaction is expected to be more pronounced for long molecules and to favor highly ordered structures. This can lead to a multitude of phases with different tilt angles^{29,30} and adsorption patterns.^{31–34}

The problem of molecular level alignment in molecule–metal junctions is one of the fundamental challenges for first-principles quantum transport simulations. On the one hand, conventional methods based on density functional theory (DFT) suffer from the problem that DFT tends to underestimate energy band gaps.³⁵ On the other hand, the widely used local DFT functionals do not correctly capture the image charge effects, which reduces the energy gaps of molecules when adsorbed on metal surfaces.^{36–38} In general, the GW approach³⁹ is currently one of the most accurate, but computationally expensive, techniques used to get quantitative agreement with experiments in the calculation of band gaps and band alignment.⁴⁰ A simpler, physically motivated correction for the errors in the Kohn–Sham orbital energies, limited to cases of relatively weak metal–molecule interactions, has also been devised and shown to provide good agreement with experimental data.^{22,41} However, in this study, we do not aim for addressing these fundamental limitations of a DFT-based treatment of the electronic structure. Instead, we will focus on another important aspect, namely, on how variations in metal–molecule junction geometry can give rise to significant shifts of the molecular level due to the electrostatics associated with interface dipoles^{42–46} and thus to changes in the electronic conduction properties.

Recently some of us showed that the inclination of alkanethiolates in a self-assembled monolayer controls the interface dipole and that the molecular level alignment can be modified by changing the tilt angle of the molecules in the film.¹⁴ On the basis of the idea of this molecular gating effect it is interesting to explore other molecular junctions where this effect would be more pronounced. Along this path, recent work on metal/organic interfaces pointed out that amine-terminated alkanes over gold possess a significantly larger effective dipole at the electrode/molecule interface than thiol-terminated alkanes.⁴⁴

Here we perform a comparative study of the role of interface dipoles for the transport through molecular films of alkanedithiolates (DT) and alkanediamines (DA) as a function of tilt. We show that these two common anchoring groups have quite different tilt-angle dependencies of the electronic and conduction properties. We present an analysis of the different band alignment processes to clarify the findings. In particular, for DT, the molecular gating can be understood and controlled by the orientation of an effective molecular dipole associated with the S–C bond. The DAs, on the contrary, are also strongly affected by charge rearrangements in the metal–molecule bond, which leads to a more complex tilt dependence.

METHODS

We performed first-principles calculations of the zero-bias conductance for the thiol- and amino-terminated self-assembled monolayer using the code TranSIESTA^{47,48} based on DFT in combination with nonequilibrium Green's functions (NEGF). To describe the scattering region of the molecular film we used unit cells containing one molecule anchored to Au(111) surfaces via gold adatoms on hollow sites, as shown in Figure 1. We note

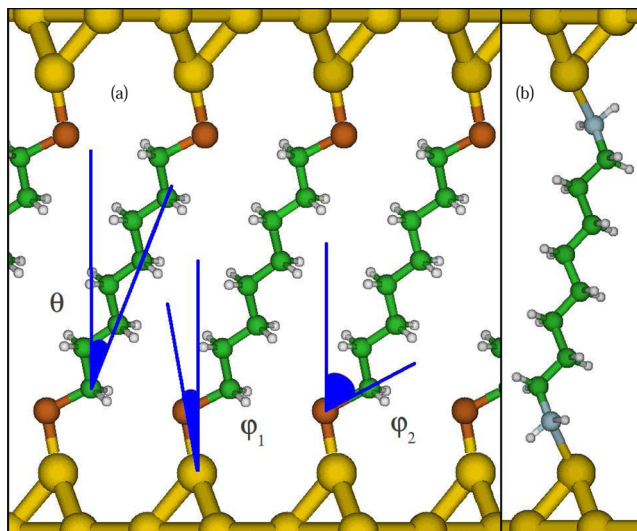


Figure 1. Definition of geometric parameters of the molecular junctions. The molecular tilt angle θ is the angle between the molecular principal axis and the surface normal. (a) Film of C8-DT molecule and corresponding angles that characterize its orientation. The angles φ_1 and φ_2 are the S-adatom–normal and C–S–normal angles, respectively. (b) C8-DA molecule anchored to Au adatoms with NH_2 groups. In this case, φ_1 and φ_2 are the N-adatom–normal and C–N–normal angles, respectively.

that while the binding to undercoordinated atoms is justified for the amines^{20,22} the same choice for the thiols is out of convenience to be able to compare similar geometries for both anchoring groups. By defining a surface unit cell of 2×2 gold atoms for each molecule we fix a molecular coverage similar to usual experimental conditions.^{29,30,49–51}

The electronic structure calculations and the relaxations are performed over a real-space grid of 200 Ry using a double- ζ plus polarization (DZP) basis for the C, S, H, and N atoms and a single- ζ plus polarization (SZP) basis for Au. We used the default energy shift value of 0.02 Ry. The molecule, the two adatoms, and the topmost Au surface layers were relaxed until residual forces were lower than 0.02 eV/Å. The remaining three Au layers at each side of the scattering region were kept fixed at bulk coordinates corresponding to a lattice constant of $a = 4.18$ Å. We used the GGA-PBE exchange-correlation functional⁵² and a Brillouin zone sampling of $5 \times 5 \times 1$ k points. Projected density of states (PDOS) onto basis orbitals were carried out using $30 \times 30 \times 1$ k points and a smearing of 0.2 eV. The transmission functions were calculated with a sampling of 32×32 k points.

We considered four different molecules, namely, butanedithiol (C4-DT), octanedithiol (C8-DT), butanediamine (C4-DA), and octanediamine (C8-DA). Furthermore, for each of these molecules we searched for three stable geometries with different tilt angles θ (defined in Figure 1). Starting from the most straight configurations, the tilted ones were generated by rigidly rotating

Table 1. Geometric and Electrostatic Properties of the Alkane Junctions^a

molecule	θ (deg tilt)	$\varphi_{18,l}$ (deg)	$\varphi_{1,u}$ (deg)	$\varphi_{2,l}$ (deg)	$\varphi_{2,u}$ (deg)	E_{HOMO} (eV)	ΔV (eV)	ΔU (eV)
C4-DT	0	18	18	39	39	-3.22	-1.75	1.67
	29	21	13	52	57	-3.14	-1.51	1.69
	38	18	19	58	61	-3.02	-1.35	1.64
C8-DT	0	22	22	43	43	-3.05	-1.61	1.67
	26	11	11	63	63	-2.81	-1.09	1.65
	35	15	5	78	75	-2.44	-0.52	1.65
C4-DA	9	22	23	40	40	-7.00	-1.17	-2.44
	26	62	62	17	17	-5.27	0.11	-1.25
	46	60	60	62	62	-4.97	-0.36	-1.01
C8-DA	14	37	36	25	26	-6.14	-0.36	-2.07
	36	14	15	43	43	-6.54	-1.15	-2.15
	42	61	61	96	96	-4.57	-0.39	-0.84

^aColumns correspond to molecular tilt angle θ , anchoring group angles φ_1 and φ_1 (defined in Figure 1) for both the lower (subscript l) and upper (subscript u) interfaces, position of HOMO level E_{HOMO} (defined in Figure 2), potential difference ΔV arising from the lower anchoring group (defined in Figure 4), and renormalization potential ΔU induced by the metal–molecule bond formation (defined in Figure 7).

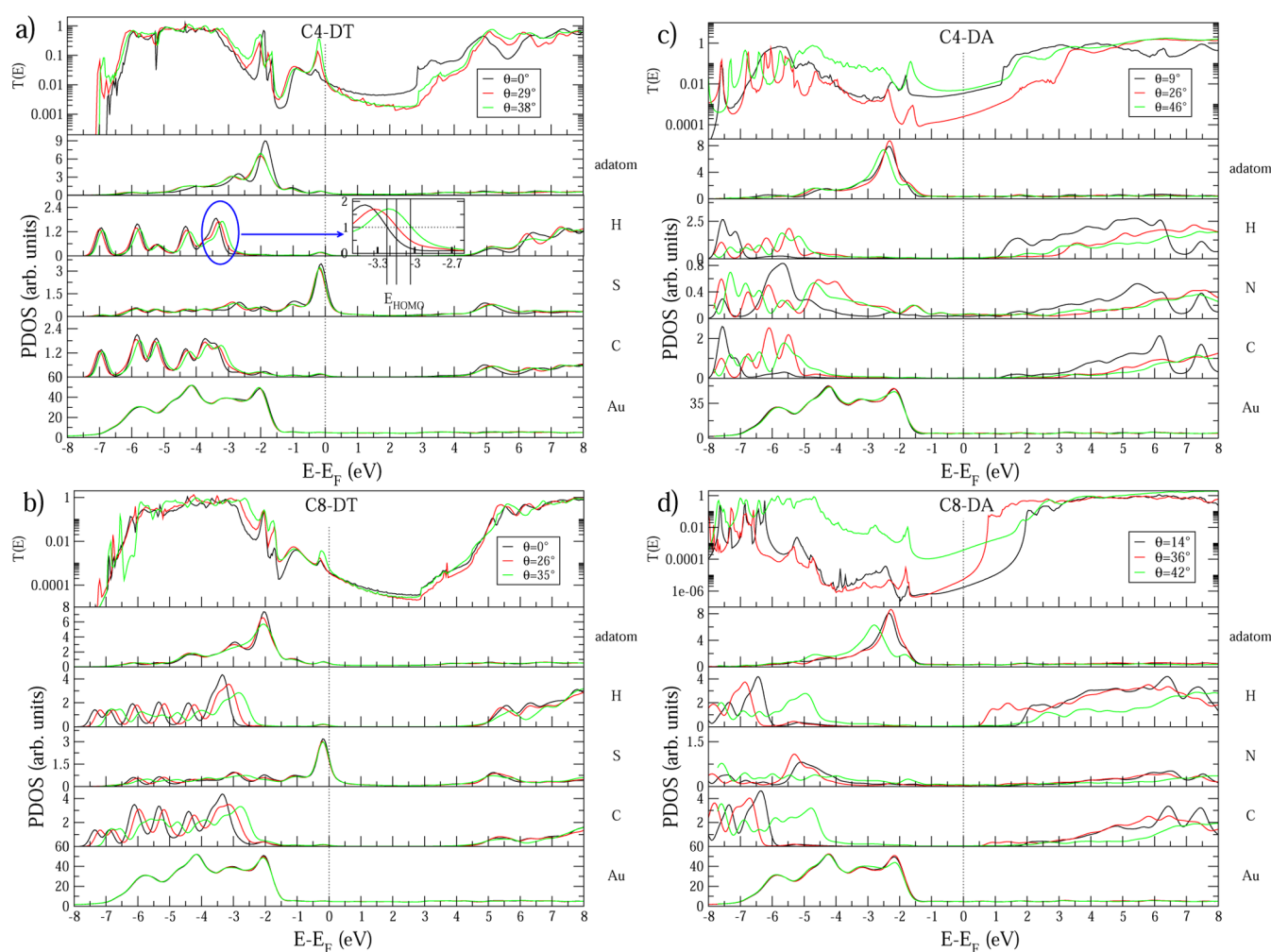


Figure 2. Electron transmission function ($T(E)$, top panel) and projected density of states (PDOS, lower panels) onto different atomic orbitals for (a) butanedithiol (C4-DT), (b) octanedithiol (C8-DT), (c) butanediamine (C4-DA), and (d) octanediamine (C8-DA) at three different tilt angles θ . The inset in panel a illustrates how we define the position of the HOMO level from the edge of the H PDOS.

the whole molecule with respect to one of the adatoms. On the other side of the junction the adatom, to which the molecule is connected, was placed on the nearest hollow site over the ideal Au(111) surface and the electrode separation was reduced accordingly. Subsequently the molecule, the two adatoms, and the topmost gold layers were relaxed until residual forces were

below 0.02 eV/Å. The results of this approach lead to a certain variation in the orientation of the anchoring groups with respect to the metal surface. We characterize this variation by the angles φ_1 and φ_2 , as defined in Figure 1, which turn out to be essential geometric parameters to describe the electronic properties of the metal–molecule interface. Actually, because the junctions at the

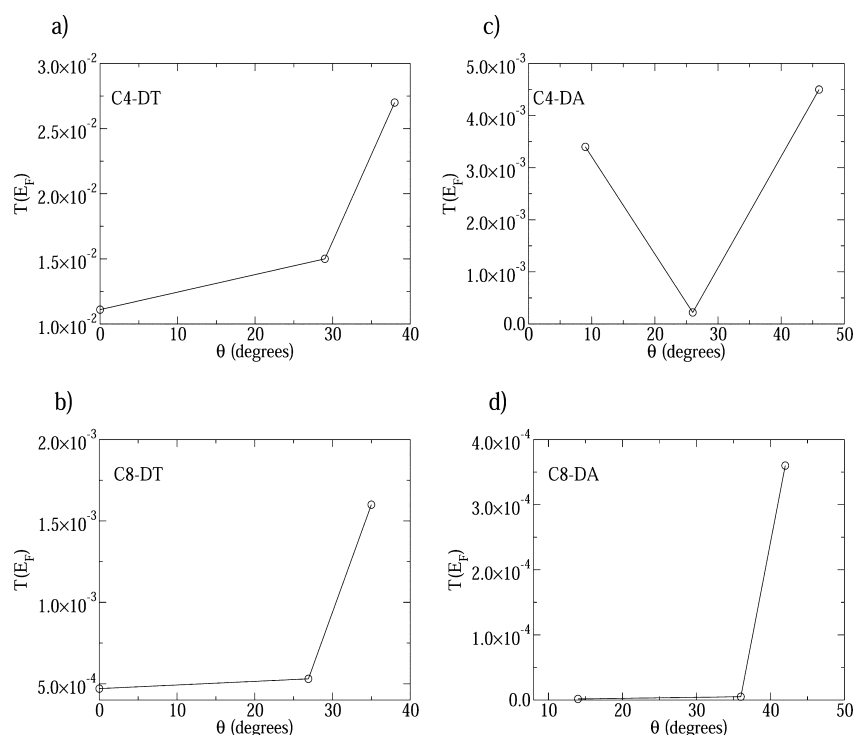


Figure 3. Transmission probability $T(E_F)$ at the Fermi energy E_F as function of molecular tilt angle θ for (a) C4-DT, (b) C8-DT, (c) C4-DA, and (d) C8-DA.

two ends of the molecule are not strictly mirror symmetric, these two parameters could differ from one side to the other. All geometric parameters are listed in Table 1.

RESULTS

Alkanedithiolates. In Figure 2a,b we present a PDOS analysis and transmission functions for C4-DT and C8-DT for different tilt angles θ with respect to the surface normal. The results are in good agreement with similar calculations¹⁴ and two-photon photoemission spectroscopy experiments⁵¹ on longer alkanes. The transmission coefficient of the alkanedithiolate junctions presents the characteristic bandgap of an alkane chain of ~ 8 eV (observed between -3 and 5 eV). The HOMO and LUMO levels are revealed in the PDOS onto H and C orbitals in Figure 2 (i.e., PDOS onto the alkane backbone). In general, the molecular levels shift upward with inclination, but they do not shift the same amount. In fact, while the HOMO is well-confined to the molecule (due to its low energetic position), the LUMO, which is higher in energy, is spatially more extended and thus couples more strongly to the metal. Therefore, the LUMO resonance is broader than the HOMO, and it does not show a well-defined shape. Furthermore, the DFT error in the HOMO position for an adsorbed molecule has been shown to be smaller than that for the LUMO.⁵³ For these reasons, in what follows we always refer to the HOMO position when discussing the molecular level alignment as a function of tilt. We define its shift in terms of the edge of the H PDOS, as illustrated in the inset in Figure 2a.

Metal and anchoring group states introduce features inside the gap of the alkane chain. At $E - E_F \approx -2$ eV the gold adatom introduces a clear resonance in the PDOS for both C4-DT and C8-DT. Similarly, the sulfur atom introduces a resonance just below the Fermi level, and this resonance may or may not show up in the junction transmission. The precise conditions for

having the S-resonance in $T(E)$ is unclear, but it appears to be very sensitive to details in the geometry. With tilt of the molecular layer this peak generally becomes more prominent. The zero-bias conductance versus tilt, shown in Figure 3a,b, is thus not purely controlled by the energy difference from the Fermi level to the HOMO position. Also, as already demonstrated in a previous work,¹⁴ the formation of intermolecular pathways for current could lead to a significant increase in conduction at Fermi level. Despite these additional complications, here we will focus on the shift of the molecular levels as one of the primary sources of changes in the transport characteristics.

Typical calculations of the tunneling decay constant β employ a series of conduction data assuming equivalent molecular conformations, where the only geometrical variable is the length of the molecular chain. In our case, with only two molecular lengths (C4 and C8), as well as due to variations in tilt, metal/molecule interfaces, and conformation of the chains, an accurate determination of β is difficult. In fact, it depends on each of these degrees of freedom. However, for the thiols we can estimate $\beta = 0.5 \text{ \AA}^{-1}$ based on C4-DT at $\theta = 0^\circ$ and C8-DT at $\theta = 0^\circ$ (the case with most equivalent geometries) which is comparable to values from the literature.¹⁹

Alkandiamines. Contrary to the case of the alkanedithiolates, our alkandiamine monolayers have the LUMO level of the carbon backbone closer to the Fermi level than the HOMO, cf. Figure 2c,d. This result is in qualitative agreement with previous calculations,⁴⁰ where it was also shown that the band alignment strongly depends on the density of the monolayer.

Comparing the PDOS in Figure 2, we can see that the molecular level shifts are much more extreme for the amines than for the thiolates. However, these shifts do not occur in a monotonous way as a function of the tilt angle. This is most clearly observed in the HOMO shift for C8-DA: an initial

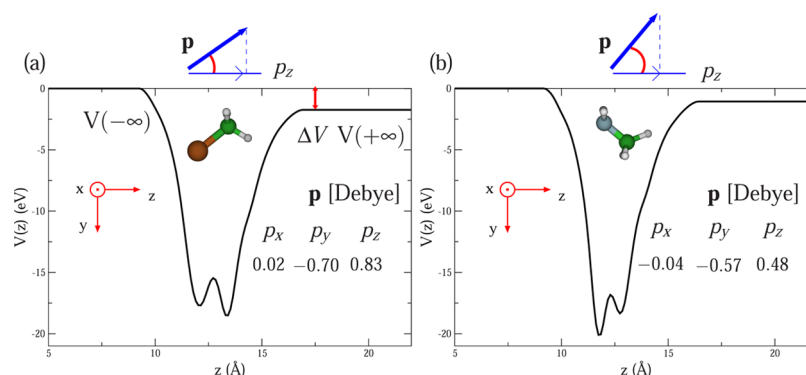


Figure 4. Plane-integrated electrostatic potential of the lower (a) thiol (SCH_3)- and (b) amine ($\text{NH}_2\text{-CH}_3$)-saturated fragments with coordinates taken from the C4-DT ($\theta = 0^\circ$) and C4-DA ($\theta = 9^\circ$) configurations, respectively. The difference between left and right vacuum levels ΔV is proportional to the z projection of molecular dipole p_z , cf. eq 1. The inset reports the numerical values of the three components of the dipole of the fragments calculated with SIESTA. The angle between the dipole and S–C (N–C) bond is found to be 1° (90°).

downshift is followed by large upshift with tilt. Another difference with respect to the thiolates is the fact that the states localized on the NH_2 group are not present near the Fermi energy.

$\text{NH}_2\text{-Au}$ bond is significantly weaker than the S–Au bond and, in the case of off-resonant transport, we would naively expect that the conductance of amine-linked molecule is lower. This is consistent with the results reported in Figure 3. While for thiolates the conductance shows a monotonous increase with tilt (Figure 3a,b), there is no such clear behavior for the amines (Figure 3c,d). Indeed this reflects a more complex dependence of the conductance on the tilt angle. Because of the geometric variations among C4-DA and C8-DA (cf. Table 1), we will not attempt to obtain a value for the effective tunneling decay constant β for the amines. As described in detail below, small differences in the geometry of the interface can strongly influence the band alignment and, therefore, the transport properties.

DISCUSSION

To rationalize the results of the previous section, in particular, the electrostatics behind the molecular level alignment, we distinguish between two components of the interface dipole: one due to the intrinsic dipole associated with the anchoring group and another one that arises due to charge redistribution due to the metal–molecule bond. In the following we analyze each of the two dipole contributions separately.

Dipole of the Anchoring Group. We start by considering the dipole that can be clearly associated with the molecule itself. Because hydrocarbons do not show any intrinsic dipolar moment,⁵⁴ the only contribution to a molecular dipole—for both thiolates and amines—must come from the anchoring group. To quantify such a dipole we considered the electrostatic potential through a layer formed by only anchoring groups. More specifically, we calculated the plane-averaged one-electron potential $V(z) = \int dx dy V(x,y,z)/A$ along the z direction with coordinates for the anchoring groups (SCH_3 for alkanedithiolates and NH_2CH_3 for alkanediamines) taken from each of the full junction geometries. We note that an extra hydrogen atom was attached to carbon and relaxed to maintain the sp^3 hybridization in the alkanes. Also, a small potential energy correction was introduced to cancel the electric field generated by the molecular dipole,⁵⁵ which otherwise would lead to interactions between the periodic repetitions of the unit cell in the z direction.

Two examples of this procedure are shown in Figure 4 for fragments of SCH_3 and NH_2CH_3 . The potential energy difference ΔV between the vacuum levels at the two sides of the anchoring group is proportional to the z projection of molecular dipole p_z ⁵⁶

$$\Delta V = V(\infty) - V(-\infty) = \frac{ep_z}{\epsilon_0 A} \quad (1)$$

where e is the elementary positive charge, ϵ_0 is the vacuum permittivity, and A is the area per unit cell in the xy plane. A negative value of ΔV thus corresponds to a positive projection of the dipole onto the z axis, that is, a projection oriented from the anchoring element (S or N) toward the C atom.

The calculated potential difference ΔV for each orientation of the anchoring groups is listed in Table 1. For the thiolates the z projection of the dipole is systematically reduced with tilt. This is consistent with the presence of a molecular dipole directed from the S atom toward the C atom.¹⁴ In fact, we confirmed that for 12 differently oriented SCH_3 fragments with coordinates derived from each of the thiol junctions, such as the one shown in Figure 4a, the angle between the calculated dipole and the S–C bond is always below 2° . This is a consequence of rotational symmetry along the S–C bond. As a result ΔV depends linearly on $\cos(\varphi_2)$, as shown in Figure 5.

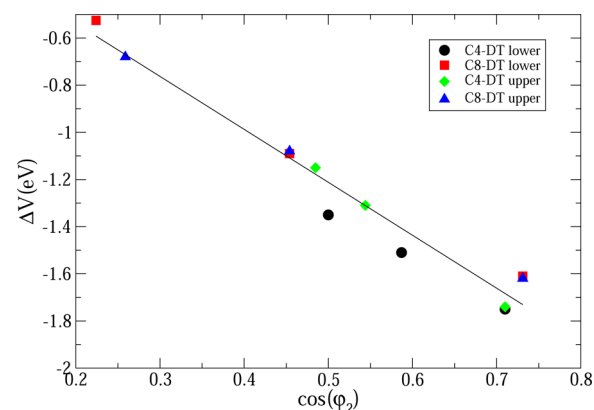


Figure 5. Plane-integrated potential drop difference ΔV over the lower and upper thiol group with respect to $\cos(\varphi_2)$ calculated for isolated molecular fragments as explained in the text. The linear regression [full line, slope of -2.2 eV] indicates that ΔV originates in a dipole aligned along the S–C bond.

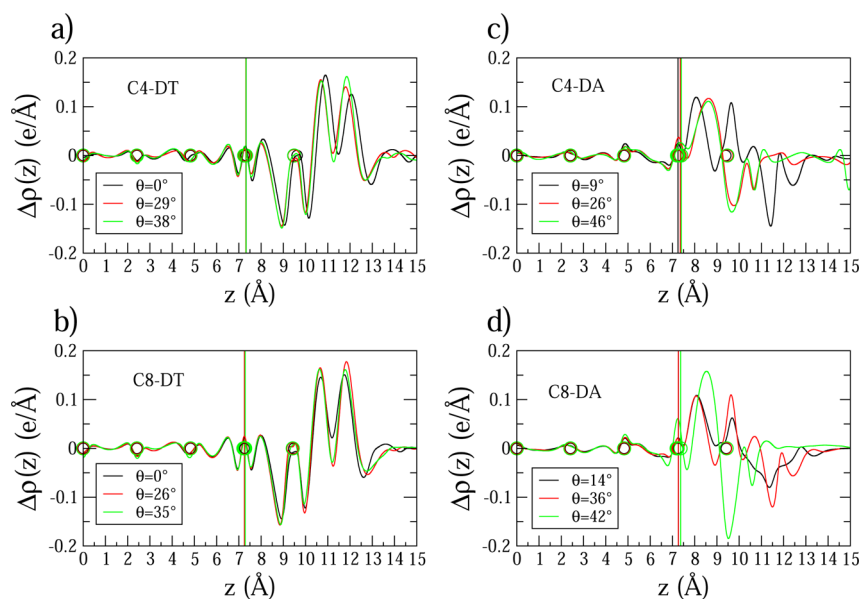


Figure 6. Plane-integrated induced electron density in the lower junction for (a) C4-DT, (b) C8-DT, (c) C4-DA, and (d) C8-DA for three different tilt angles θ . In the case of amines the shifts of the electron density can be understood in terms of the N-adatom-normal angle φ_1 . Vertical lines indicate the position of the Au(111) surface. The circles represent the Au atoms, with the rightmost circle being the Au adatom.

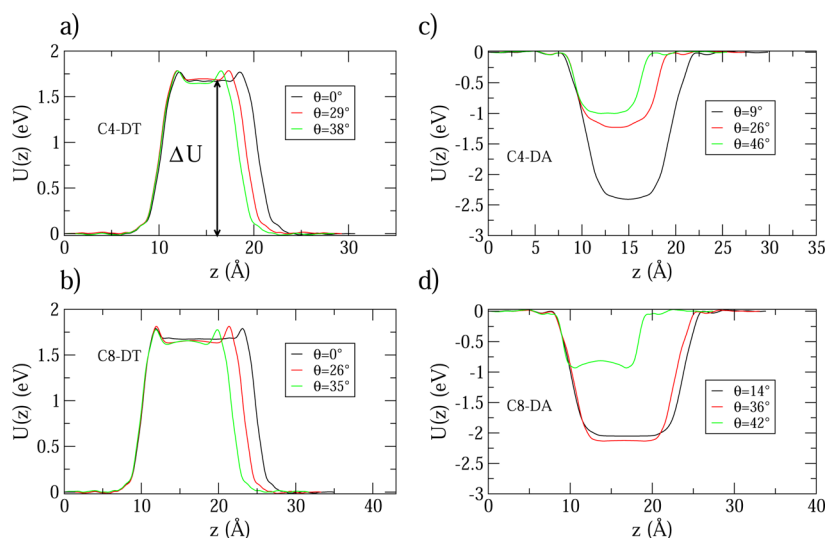


Figure 7. Calculated renormalization potential $U(z)$ for (a) C4-DT, (b) C8-DT, (c) C4-DA, and (d) C8-DA at three different tilt angles θ . The potential difference ΔU is measured in the middle of the molecular film, as shown in panel a.

In the case of amines the situation is more complex. The angle between the calculated dipole and the N–C bond for 12 differently oriented NH_2CH_3 fragments with coordinates derived from each of the amine junctions, such as the one shown in Figure 4b, varied in the range $80\text{--}90^\circ$. This follows naturally from the fact that there is no rotational symmetry along the N–C bond for the amine fragments. The molecular dipole, approximately perpendicular to the N–C bond, is therefore not uniquely characterized by φ_2 . As a result ΔV does not scale linearly with $\cos(\varphi_2)$ (not shown).

Charge Redistribution Due to Metal–Molecule Bond.

Next we look into the other contribution to the interface dipole, namely, that arising from charge redistribution due to the metal–molecule bond. To quantify this, we considered the plane-integrated electron density difference $\Delta\rho(z)$ that results from the interaction between the metal and molecular subsystems, that is

$$\Delta\rho(z) = \rho_{\text{sys}}(z) - [\rho_{\text{SAM}}(z) + \rho_{\text{metal}}(z)] \quad (2)$$

where $\rho_{\text{sys}}(z)$ is the electron density of the metal/molecule/metal system while $\rho_{\text{SAM}}(z)$ and $\rho_{\text{metal}}(z)$ are the electron densities for the isolated SAM and metal subsystem, respectively.

The charge redistribution $\Delta\rho(z)$, due to the metal–molecule bond, is shown in Figure 6. It generates a potential difference for the electrons ΔU over the interface that satisfies the Poisson equation

$$\nabla^2 U = -\frac{e}{\epsilon_0} \Delta\rho(z) \quad (3)$$

The corresponding electrostatic potentials $U(z)$ are shown in Figure 7, and the differences ΔU for each geometry are listed in Table 1. We note that ΔU is positive (negative) for the thioliates (amines), which reflects an electron accumulation (depletion) on the anchoring group. This difference implies higher-lying

molecular levels for the thiolates than for the amines. We return to this issue in the next section.

The charge redistribution originates from a series of complex metal–molecule interactions whose effects are difficult to separate. In the case of thiolates (Figure 6a,b) there are no appreciable changes with tilt. However, for the amines (Figure 6c,d), two effects appear when tilt increases. Analyzing the induced charge averaged over the xy plane, we find that: (i) the accumulation of electron density appearing right over the surface shifts slightly toward the molecular layer and (ii) an electron density depletion region moves toward the adatom position.

The change in $\Delta\rho(z)$ with tilt can be explained in terms of the so-called push-back (PB) or pillow effect.^{42,43,57} In short, PB is the back-shift of the metal electrons due to the overlap with the electron cloud of the molecule due to the Pauli exclusion principle; it always results in a decrease in the metal workfunction^{45,58} as the metal–molecule bond is formed and thus in a downshift of the molecular levels with respect to the Fermi level. For the amines it can be associated with the N lone pair: when it is directed along the normal to the gold surface (small φ_1) there is a large overlap with metals states so it pushes back the electron cloud of the electrodes (black curve in Figure 6c and black/red curves in Figure 6d), reducing the metal work function and shifting down molecular levels. On the contrary, when we tilt the molecular film (large φ_1), the N lone pair is pointing away from the gold surface, and its overlap with the metal states becomes smaller. As a consequence, the PB effect is reduced and the charge density of the electrodes extends farther away from the surface (red/green curves in Figure 6c and green curve in Figure 6d). The result is a larger dipole of the metal surface and consequently also a larger work function, which results in an upward shift of the molecular levels with respect to the nontilted positions.

The second effect mentioned, namely, the electron depletion appearing at the adatom position with tilt, is due to simple geometrical reasons, as shown in Figure 8. As the tilt increases,

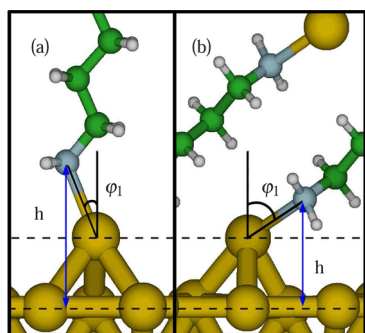


Figure 8. Distance h of the NH_2 group from the Au(111) surface for the C4-DA molecule at (a) $\theta = 9^\circ$ and (b) $\theta = 46^\circ$. This shows that h decreases with tilt and the electron depletion associated with the amine group moves closer to the metal.

the negative $\Delta\rho$ associated with the functional NH_2 group moves toward the z position of the adatom. This results in an overall reduction of the $\Delta\rho(z)$ at that height. As the NH_2 -to-surface distance h is related to $\cos(\varphi_1)$, we find a fairly linear relationship between ΔU and $\cos(\varphi_1)$, as observed in Figure 9.

Position of the HOMO Level. As explained above, the interface dipole of the various junctions is composed of two parts, namely, one related to the anchoring group and another one originating from the metal–molecule bond. To show that the

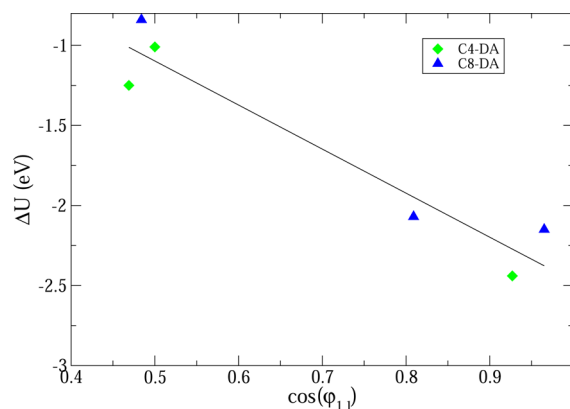


Figure 9. Change of the renormalization potential ΔU with respect to $\cos(\varphi_{1,i})$ in the case of alkanediamines. The linear regression (full line, slope of 2.8 eV) indicates that ΔU is related to the NH_2 -to-surface distance.

HOMO level position can be understood in terms of these two contributions, we plot in Figure 10 the E_{HOMO} as a function of the sum of two electrostatic potential differences ΔV and ΔU . Indeed, a very satisfactory linear dependence is observed, supporting the notion that changes in the molecular level alignment can be understood in terms of the variations in the effective interface dipole. Furthermore, this result suggests that the molecular level alignment of alkanes with other terminal groups can be estimated by considering the orientation of a dipole of the anchor in combination with the charge rearrangement that occurs during the formation of the metal–molecule bond.

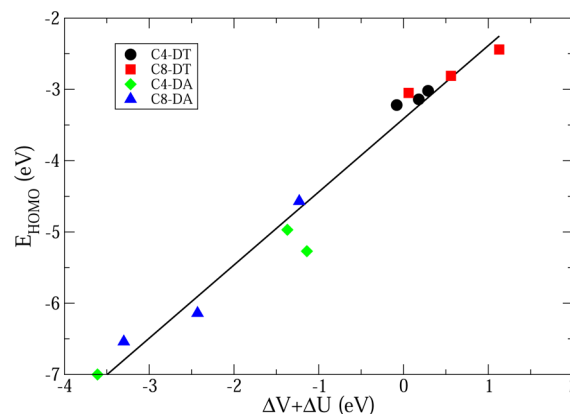


Figure 10. Change of the HOMO position E_{HOMO} with respect to the sum of the anchor group potential difference ΔV and renormalization potential ΔU . The linear regression (full line, slope of 1.0) shows that the changes in molecular level alignment can be understood in terms of variations in the effective interface dipole.

CONCLUSIONS

We have studied the molecular level alignment and conductance of thiol- and amino-terminated SAMs over Au(111) as a function of the tilt angle. We have found that the observed shifts in the molecular resonances can be rationalized in terms of electrostatic potentials set up by the effective interface dipole,¹⁴ which has two components: (i) a rigid dipole associated with the anchoring group that changes its projection on the axis perpendicular to the metal surface with tilt and (ii) a charge redistribution induced by

the formation of the metal–molecule bond. For the thiolates the level alignment is essentially only sensitive to the first effect, as the charge distribution over the S–Au bond does not show a tilt dependence. This leads to a direct dependence between the HOMO position and the tilt of the molecular film, which in turn can be considered as mechanical gating of the electron transport through the SAM. (The conductance increases with tilt.)

For the amines we have found that the level alignment is strongly affected by both electrostatic components. Whereas this leads to a significantly larger variation in the HOMO level position with tilt (~ 2.5 eV for amines compared with 0.8 eV for thiolates), this, unfortunately, does not provide a simple way to mechanically gate the electron transport through the molecular layer because the charge redistribution over the NH_2 –Au bond depends sensitively on other geometric parameters than the tilt angle, in particular, the orientation of the N lone pair with respect to the metal surface.

AUTHOR INFORMATION

Corresponding Author

*E-mail: giuseppe_foti@ehu.es.

Notes

The authors declare no competing financial interest.

ACKNOWLEDGMENTS

G.F. acknowledges support from the CSIC JAE-predoc program, cofinanced by the European Science Foundation. We also acknowledge the support of the Basque Departamento de Educación and the UPV/EHU (Grant No. IT-756-13), the Spanish Ministerio de Economía y Competitividad (Grant No. FIS2010-19609-CO2-00), and the ETORTEK program funded by the Basque Departamento de Industria and the Diputación Foral de Gipuzkoa. T.F. and G.F. thank Center for Nanostructured Graphene (Project DNRF58) for hospitality.

REFERENCES

- (1) Aviram, A.; Ratner, M. A. Molecular Rectifiers. *Chem. Phys. Lett.* **1974**, *29*, 277–283.
- (2) Cuevas, J. C.; Scheer, E. *Molecular Electronics - An Introduction to Theory and Experiment*; World Scientific: Singapore, 2010.
- (3) Metzger, R. M.; et al. Unimolecular Electrical Rectification in Hexadecylquinolinium Tricyanoquinodimethanide. *J. Am. Chem. Soc.* **1997**, *119*, 10455–10466.
- (4) Chen, J.; Reed, M. A.; Rawlett, A. M.; Tour, J. M. Large On-Off Ratios and Negative Differential Resistance in a Molecular Electronic Device. *Science* **1999**, *286*, 1550–1552.
- (5) van der Molen, S. J.; Liljeroth, P. Charge Transport through Molecular Switches. *J. Phys.: Condens. Matter* **2010**, *22*, 133001.
- (6) Smit, R. H. M.; Noat, Y.; Untiedt, C.; Lang, N. D.; van Hemert, M. C.; van Ruitenbeek, J. M. Measurement of the Conductance of a Hydrogen Molecule. *Nature (London)* **2002**, *419*, 906–909.
- (7) Kubatkin, S.; Danilov, A.; Hjort, M.; Cornil, J.; Bredas, J. L.; Stuhr-Hansen, N.; Hedegård, P.; Bjørnholm, T. Single-Electron Transistor of a Single Organic Molecule with Access to Several Redox States. *Nature (London)* **2003**, *425*, 698–701.
- (8) Ulman, A. Formation and Structure of Self-Assembled Monolayers. *Chem. Rev.* **1996**, *96*, 1533–1554.
- (9) Love, J. C.; Estroff, L. A.; Kriebel, J. K.; Nuzzo, R. G.; Whitesides, G. M. Self-Assembled Monolayers of Thiolates on Metals as a Form of Nanotechnology. *Chem. Rev.* **2005**, *105*, 1103–1170.
- (10) Kind, M.; Wöll, C. Organic Surfaces Exposed by Self-Assembled Organothiol Monolayers: Preparation, Characterization, and Application. *Prog. Surf. Sci.* **2009**, *84*, 230–278.
- (11) Ulrich, J.; Esrail, D.; Pontius, W.; Venkataraman, L.; Millar, D.; Doerr, L. H. Variability of Conductance in Molecular Junctions. *J. Phys. Chem. B* **2006**, *110*, 2462–2466.
- (12) Sen, A.; Kaun, C.-C. Effect of Electrode Orientations on Charge Transport in Alkanedithiol Single-Molecule Junctions. *ACS Nano* **2010**, *4*, 6404–6408.
- (13) Pauly, F.; Viljas, J. K.; Cuevas, J. C.; Schön, G. Density-Functional Study of Tilt-Angle and Temperature-Dependent Conductance in Biphenyl Dithiol Single-Molecule Junctions. *Phys. Rev. B* **2008**, *77*, 155312.
- (14) Frederiksen, T.; Munuera, C.; Ocal, C.; Brandbyge, M.; Paulsson, M.; Sánchez-Portal, D.; Arnau, A. Exploring the Tilt-Angle Dependence of Electron Tunneling across Molecular Junctions of Self-Assembled Alkanethiols. *ACS Nano* **2009**, *3*, 2073–2080.
- (15) Paulsson, M.; Krag, C.; Frederiksen, T.; Brandbyge, M. Conductance of Alkanedithiol Single-Molecule Junctions: A Molecular Dynamics Study. *Nano Lett.* **2009**, *9*, 117–121.
- (16) Kim, Y.; Song, H.; Strigl, F.; Pernau, H.-F.; Lee, T.; Scheer, E. Conductance and Vibrational States of Single-Molecule Junctions Controlled by Mechanical Stretching and Material Variation. *Phys. Rev. Lett.* **2011**, *106*, 196804.
- (17) Cui, X. D.; Primak, A.; Zarate, X.; Tomfohr, J.; Sankey, O. F.; Moore, A. L.; Moore, T. A.; Gust, D.; Harris, G.; Lindsay, S. M. Reproducible Measurement of Single-Molecule Conductivity. *Science* **2001**, *294*, 571–574.
- (18) Jiang, J.; Lu, W.; Luo, Y. Length Dependence of Coherent Electron Transportation in Metal-Alkanedithiol-Metal and Metal-Alkanemonthiol-Metal Junctions. *Chem. Phys. Lett.* **2004**, *400*, 336–340.
- (19) Li, C.; Pobelov, I.; Wandlowski, T.; Bagrets, A.; Arnold, A.; Evers, F. Charge Transport in Single Au/Alkanedithiol/Au Junctions: Coordination Geometries and Conformational Degrees of Freedom. *J. Am. Chem. Soc.* **2008**, *130*, 318–326.
- (20) Venkataraman, L.; Klare, J. E.; Tam, I. W.; Nuckolls, C.; Hybertsen, M. S.; Steigerwald, M. L. Single-Molecule Circuits with Well-Defined Molecular Conductance. *Nano Lett.* **2006**, *6*, 458–462.
- (21) Chen, F.; Li, X.; Hihath, J.; Huang, Z.; Tao, N. J. Effect of Anchoring Groups on Single-Molecule Conductance: Comparative Study of Thiol-, Amine-, and Carboxylic-Acid-Terminated Molecules. *J. Am. Chem. Soc.* **2006**, *128*, 15874–15881.
- (22) Quek, S. Y.; Venkataraman, L.; Choi, H. J.; Louie, S. G.; Hybertsen, M. S.; Neaton, J. B. Amine-Gold Linked Single-Molecule Circuits: Experiment and Theory. *Nano Lett.* **2007**, *7*, 3477–3482.
- (23) Fagas, G.; Greer, J. C. Tunneling in Alkanes Anchored to Gold Electrodes via Amine End Groups. *Nanotechnology* **2007**, *18*, 424010.
- (24) Prodan, E.; Car, R. Tunneling Conductance of Amine-Linked Alkyl Chains. *Nano Lett.* **2008**, *8*, 1771–1777.
- (25) McDermott, S.; George, C. B.; Fagas, G.; Greer, J. C.; Ratner, M. A. Tunnel Currents across Silane Diamines/Dithiols and Alkane Diamines/Dithiols: A Comparative Computational Study. *J. Phys. Chem. C* **2009**, *113*, 744–750.
- (26) Kim, Y.; Hellmuth, T. J.; Bürkle, M.; Pauly, F.; Scheer, E. Characteristics of Amine-Ended and Thiol-Ended Alkane Single-Molecule Junctions Revealed by Inelastic Electron Tunneling Spectroscopy. *ACS Nano* **2011**, *5*, 4104–4111.
- (27) Cheng, Z.-L.; Skouta, R.; Vazquez, H.; Widawsky, J. R.; Schneebeli, S.; Chen, W.; Hybertsen, M. S.; Breslow, R.; Venkataraman, L. In Situ Formation of Highly Conducting Covalent Au-C Contacts for Single-Molecule Junctions. *Nat. Nanotechnol.* **2011**, *6*, 353–357.
- (28) Vericat, C.; Vela, M. E.; Benitez, G.; Carro, P.; Salvarezza, R. C. Self-Assembled Monolayers of Thiols and Dithiols on Gold: New Challenges for a Well-Known System. *Chem. Soc. Rev.* **2010**, *39*, 1805–1834.
- (29) Barrera, E.; Ocal, C.; Salmeron, M. Structure and Stability of Tilted-Chain Phases of Alkanethiols on Au(111). *J. Chem. Phys.* **2001**, *114*, 4210–4214.
- (30) Wang, Y.; Solano-Canchaya, J. G.; Alcamí, M.; Busnengo, H. F.; Martín, F. Commensurate Solid-Solid Phase Transitions in Self-

Assembled Monolayers of Alkylthiolates Lying on Metal Surfaces. *J. Am. Chem. Soc.* **2012**, *134*, 13224–13227.

(31) Kato, H. S.; Noh, J.; Hara, M.; Kawai, M. An HREELS Study of Alkanethiol Self-Assembled Monolayers on Au(111). *J. Phys. Chem. B* **2002**, *106*, 9655–9658.

(32) Yu, M.; Bovet, N.; Satterley, C. J.; Bengió, S.; Lovelock, K. R. J.; Milligan, P. K.; Jones, R. G.; Woodruff, D. P.; Dhanak, V. True Nature of an Archetypal Self-Assembly System: Mobile Au-Thiolate Species on Au(111). *Phys. Rev. Lett.* **2006**, *97*, 166102.

(33) Tao, F.; Bernasek, S. L. Understanding Odd-Even Effects in Organic Self-Assembled Monolayers. *Chem. Rev.* **2007**, *107*, 1408–1453.

(34) Chaudhuri, A.; Lerotholi, T. J.; Jackson, D. C.; Woodruff, D. P.; Dhanak, V. Local Methylthiolate Adsorption Geometry on Au(111) from Photoemission Core-Level Shifts. *Phys. Rev. Lett.* **2009**, *102*, 126101.

(35) Godby, R. W.; Schlüter, M.; Sham, L. J. Accurate Exchange-Correlation Potential for Silicon and Its Discontinuity on Addition of an Electron. *Phys. Rev. Lett.* **1986**, *56*, 2415.

(36) Neaton, J. B.; Hybertsen, M. S.; Louie, S. G. Renormalization of Molecular Electronic Levels at Metal-Molecule Interfaces. *Phys. Rev. Lett.* **2006**, *97*, 216405.

(37) Thygesen, K. S.; Rubio, A. Renormalization of Molecular Quasiparticle Levels at Metal-Molecule Interfaces: Trends across Binding Regimes. *Phys. Rev. Lett.* **2009**, *102*, 046802.

(38) Kaasbjerg, K.; Flensberg, K. Strong Polarization-Induced Reduction of Addition Energies in Single-Molecule Nanojunctions. *Nano Lett.* **2008**, *8*, 3809–3814.

(39) Hedin, L. New Method for Calculating the One-Particle Green's Function with Application to the Electron-Gas Problem. *Phys. Rev.* **1965**, *139*, A796–A823.

(40) Strange, M.; Thygesen, K. S. Towards Quantitative Accuracy in First-Principles Transport Calculations: The GW Method Applied to Alkane/Gold Junctions. *Beilstein J. Nanotechnol.* **2011**, *2*, 746–754.

(41) Dell-Angela, M.; Kladnik, G.; Cossaro, A.; Verdini, A.; Kamenetska, M.; Tamblyn, I.; Quek, S. Y.; Neaton, J. B.; Cvetko, D.; Morgante, A.; Venkataraman, L. Relating Energy Level Alignment and Amine-Linked Single Molecule Junction Conductance. *Nano Lett.* **2010**, *10*, 2470–2474.

(42) Vazquez, H.; Dappe, Y.; Ortega, J.; Flores, F. A Unified Model for Metal/Organic Interfaces: IDIS, Pillow Effect and Molecular Permanent Dipoles. *Appl. Surf. Sci.* **2007**, *254*, 378–382.

(43) Vazquez, H.; Dappe, Y. J.; Ortega, J.; Flores, F. Energy Level Alignment at Metal/Organic Semiconductor Interfaces: “Pillow” Effect, Induced Density of Interface States, and Charge Neutrality Level. *J. Chem. Phys.* **2007**, *126*, 144703.

(44) Wang, J.-G.; Prodan, E.; Car, R.; Selloni, A. Band Alignment in Molecular Devices: Influence of Anchoring Group and Metal Work Function. *Phys. Rev. B* **2008**, *77*, 245443.

(45) Heimel, G.; Romaner, L.; Zojer, E.; Bredas, J.-L. The Interface Energetics of Self-Assembled Monolayers on Metals. *Acc. Chem. Res.* **2008**, *41*, 721–729.

(46) Rousseau, R.; De Renzi, V.; Mazzarello, R.; Marchetto, D.; Biagi, R.; Scandolo, S.; del Pennino, U. Interfacial Electrostatics of Self-Assembled Monolayers of Alkane Thioliates on Au(111): Work Function Modification and Molecular Level Alignments. *J. Phys. Chem. B* **2006**, *110*, 10862–10872.

(47) Soler, J. M.; Artacho, E.; Gale, J. D.; García, A.; Junquera, J.; Ordejón, P.; Sánchez-Portal, D. The SIESTA Method for Ab Initio Order-N Materials Simulation. *J. Phys.: Condens. Matter* **2002**, *14*, 2745–2779.

(48) Brandbyge, M.; Mozos, J. L.; Ordejón, P.; Taylor, J.; Stokbro, K. Density-Functional Method for Nonequilibrium Electron Transport. *Phys. Rev. B* **2002**, *65*, 165401.

(49) Barrera, E.; Palacios-Lidon, E.; Munuera, C.; Torrelles, X.; Ferrer, S.; Jonas, U.; Salmeron, M.; Ocal, C. The Role of Intermolecular and Molecule-Substrate Interactions in the Stability of Alkanethiol Non-saturated Phases on Au(111). *J. Am. Chem. Soc.* **2004**, *126*, 385–395.

(50) Smaali, K.; Clément, N.; Patriarche, G.; Vuillaume, D. Conductance Statistics from a Large Array of Sub-10 nm Molecular Junctions. *ACS Nano* **2012**, *6*, 4639–4647.

(51) Hirata, N.; Shibuta, M.; Matsui, R.; Nakajima, A. Electronic States of Alkanethiolate Self-Assembled Monolayers on Au(111) Studied by Two-Photon Photoemission Spectroscopy. *J. Phys. Chem. C* **2012**, *116*, 13623.

(52) Perdew, J. P.; Burke, K.; Ernzerhof, M. Generalized Gradient Approximation Made Simple. *Phys. Rev. Lett.* **1996**, *77*, 3865–3868.

(53) Garcia-Lastra, J. M.; Rostgaard, C.; Rubio, A.; Thygesen, K. S. Polarization-Induced Renormalization of Molecular Levels at Metallic and Semiconducting Surfaces. *Phys. Rev. B* **2009**, *80*, 245427.

(54) Fox, M. A.; Whitesell, J. K. *Organic Chemistry*; Jones and Bartlett Publisher: Sudbury, MA, 2004.

(55) Bengtsson, L. Dipole Correction for Surface Supercell Calculations. *Phys. Rev. B* **1999**, *59*, 12301–12304.

(56) Jackson, J. D. *Classical Electrodynamics*; Wiley: New York, 1975.

(57) Witte, G.; Lukas, S.; Bagus, P. S.; Wöll, C. Vacuum Level Alignment at Organic/Metal Junctions: “Cushion” Effect and the Interface Dipole. *Appl. Phys. Lett.* **2005**, *87*, 263502.

(58) Rusu, P. C.; Giovannetti, G.; Weijtens, C.; Coehoorn, R.; Brocks, G. First-Principles Study of the Dipole Layer Formation at Metal-Organic Interfaces. *Phys. Rev. B* **2010**, *81*, 125403.